Polymer Brushes on Flat and Curved Substrates: Scaling Concepts and Computer Simulations

Dimitar Dimitrov,[1,2] *Andrey Milchev,*[1,3] *Kurt Binder**[1]

Summary: The scaling concepts for isolated flexible macromolecules in good solvent grafted with one chain end to a flat surface (''polymer mushrooms'') as well as for layers of many overlapping end-grafted chain molecules (''polymer brushes'') are introduced. Monte Carlo attempts to test these concepts are briefly reviewed. Then the extension of these concepts to polymer brushes grafted to the interior of a cylinder surface is discussed. Molecular Dynamics results on chain average linear dimensions in the direction normal to the grafting surface and in axial direction are described, as well as distribution functions for the density of end monomers and of all monomers of the chains. It is argued that under typical conditions reachable in either simulation or experiment the data fall in a crossover regime, where no simple power-laws (as derived from the scaling description) hold. Moreover, extensions of the Daoud-Cotton blob picture to the cylinder geometry, implying that each chain in such a cylindrical brush is confined into a conical sector, are invalid; thus, chain ends in densely filled cylinders are not restricted to stay in the ''hemicylinder'' containing the grafting site of the chain.

Keywords: cylindrical pore; molecular dynamics; polymer brush; scaling theory

Introduction: Polymer Brushes on Flat Substrates

Polymer brushes have been a subject of intensive study during the last few decades, both by experiment,[1–9] theory [10–37] and simulation.[38–52] Part of this interest is due to their broad applications (for the stabilization of colloids, as lubricants, adhesives, etc.[7–9]), but this is out of scope in the present work. Here we focus on the challenging problem of the conformational statistics of polymer chains in polymer brushes (the response of brushes to shear deformation [7,8,48,49] also shall not be considered here).

Polymer brushes can be made from flexible polymers with special endgroups, which get strongly adsorbed at surfaces, while the rest of the chain has a repulsive interaction with the substrate. One may realize this situation also with a very asymmetric block copolymer, with adsorbing A-blocks that have a much smaller chain length than the non-adsorbing B-blocks, $N_A \ll N_B$. If the grafting density of the chains is so dilute, that the chains do not interact with each other, the resulting polymer configuration is called a ''mushroom''. Under very good solvent conditions the gyration radius component R_{gz} in the z-direction perpendicular to the substrate scales with the same exponent ($\nu = 0.588$[53] $\approx 3/5$) as the parallel component $R_{g\|}$ or the radius R_g in the bulk,

$$R_{gz} \propto R_{g\|} \propto R_g \propto N^{\nu} \tag{1}$$

where N is the number of (effective) monomeric units forming the chain molecule. Although in the linear dimensions of the mushroom no new exponent is involved, interesting scaling behavior is predicted [12] for the density profile $\phi(z)$,

[1] Institut für Physik, Johannes Gutenberg-Universität, D-55099 Mainz, Germany
E-mail: kurt.binder@uni-mainz.de
[2] Inorganic Chemistry and Physical Chemistry Department, University of Food Technology, Maritza Blvd. 26, 4002 Plovdiv, Bulgaria
[3] Institute of Physical Chemistry, Bulgarian Academy of Sciences, 1113 Sofia, Bulgaria

z being the distance from the substrate:

$$\frac{\phi(z)}{\phi(z=R_g)} = \tilde{F}\left(\frac{z}{R_g}\right), \quad \tilde{F}(\zeta) \propto \zeta^{\kappa}, \zeta \ll 1 \tag{2}$$

where the exponent $\kappa = 1/\nu - 1 \approx 0.7$. Kreer *et al.*[50] have verified this scaling structure for the bead spring model[54–56] that will be described in more detail in later sections of this paper, and has been used also in the context of Molecular Dynamics simulation.[38,41,43,46–49,51,52]

At high grafting densities, when the mushrooms overlap strongly, unfavorable excluded volume interactions can be avoided via stretching of the chains in the z-direction, perpendicular to the grafting surface. The simplest description (''Alexander picture''[11]) assumes a regular arrangement of grafting sites according to the grafting density σ, so that the distance between grafting sites is $\sigma^{-1/2}$, and postulates a ''blob'' picture,[23,30,57] i.e., each chain is taken to be a string of blobs of diameter $\sigma^{-1/2}$, and inside a blob excluded volume interactions are not screened: so, if there are n monomers contained in each blob, we have $\sigma^{-1/2} = n^{3/5}$, (ignoring prefactors of order unity, and ignoring also the deviation of ν from 3/5 at this point). Thus, inside a blob the same law as in a free chain holds {Equation (1)}, and hence $n = \sigma^{-5/6}$. If we assume that each chain is just a cigar-shaped string of $n_B = N/n = N\sigma^{5/6}$ blobs, the prediction for the brush height h and the chain linear dimensions become

$$h = R_{gz} = \sigma^{-1/2} n_B = \sigma^{1/3} N, \quad R_{g\|} = \sigma^{-1/2} \tag{3}$$

Actually the last of these predictions needs to be revised even within this picture, since the one-dimensional string of blobs may make transverse fluctuations, random excursions in the directions parallel to the wall, and hence

$$R_{g\|} = n_B^{1/2} \sigma^{-1/2} = \sigma^{-1/12} N^{1/2} \tag{4}$$

The density distribution $\phi(z)$ and the distribution of the free chain ends $\rho(z)$ then simply become a step function and a delta function, respectively,

$$\phi(z)/\phi(0) = \Theta(h - z), \quad \rho(z) = \sigma^{-1/2}\delta(z - h) \tag{5}$$

Note that the crossover to the mushroom behavior occurs when $n_B = 1$ (i.e., $N = n$), that is, for $\sigma = \sigma^* = N^{-6/5}$, and is smooth (then all the above linear dimensions become compatible with Equation (1) again).

However, there is ample evidence from more refined theories,[13–37] simulations,[38–44,50–52] and experiment[3–5] that the above simple description {Equation (5)} is incorrect, there is no jump discontinuity of $\phi(z)$ at $z = h$, but rather there is a smooth decrease of $\phi(z)$ with increasing z. Approximately this can be described by the strong stretching limit of the self-consistent field theory, which yields a parabolic profile[14]

$$\phi(z)/\phi(0) = 1 - (z/h)^2 \tag{6}$$

and also the chain ends are distributed over the whole brush,[14]

$$\rho(z) \propto \sigma^{-2/3} N^{-2} z[1 - (z/h)^2]^{1/2} \tag{7}$$

However, this strong stretching limit of the chains (together with the condition that the blob size is much larger than the size of a monomer, $\sigma^{-1/2} \gg 1$ (we take here the size of the monomer as a unit of length), is hardly ever reached in either experiment or simulation; rather it is typical that neither $\phi(z)$ nor $\rho(z)$ exhibit a sharp cutoff at a well-defined brush height h. Typical simulation results (for a bead-spring model that will be described below) are shown in Figure 1. It is not obvious how to give the brush height h a precise meaning from data such as shown in Figure 1 (or similar data in the earlier literature[38–40,47]). Thus it is widespread practice to define the brush height from the first moment $\langle z \rangle$ of the profile as

$$h = (8/3)\langle z \rangle, \quad \langle z \rangle = \int_0^\infty \phi(z) z dz \Big/ \int_0^\infty \phi(z)\, dz \tag{8}$$

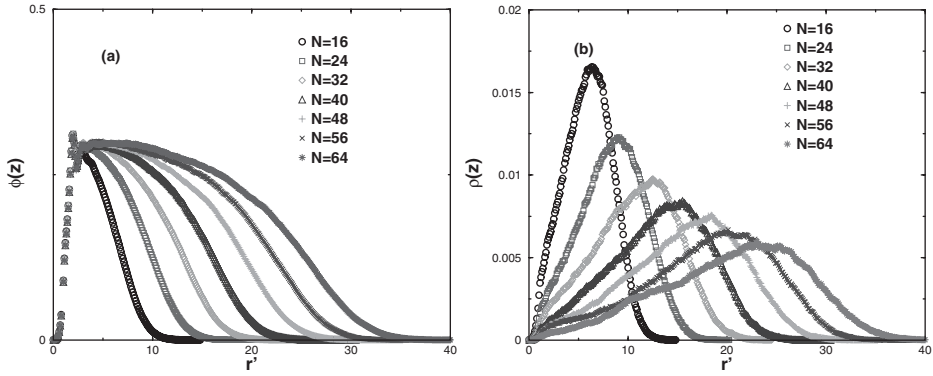

Figure 1.
Monomer density profile $\phi(z)$ versus z (a), and distribution of end monomers $\rho(z)$ versus z (b) of a polymer brush on a flat of substrate. All data refer to a grafting density $\sigma = 0.1$, grafting $N_{ch} = 324$ chains on an area $A = 3117$. Seven chain lengths N are included in the figure, as indicated.

since for the parabolic profile, Equation (6), this definition coincides with the definition $\phi(z = h) = 0$ used there.

Actually in the monomer density profile of a polymer brush there occur a multitude of length scales: very close to the (hard) wall at which the chains are grafted, one observes ''layering'', i.e. oscillations of density on the scale of the effective monomers. These effects due to the packing of monomers against the substrate clearly are model-dependent and hence non-universal and shall not be discussed here. However, apart from the brush height h itself there is also a length scale describing over which range the parabolic density profile, Equation (6), is rounded. Wittmer *et al.*[44] have proposed a non-uniform blob picture to reconcile Equation (6) with the blob concept, arguing that the screening length of the excluded volume interaction ξ scales with ϕ in a bulk semidilute solution as $\xi \propto \phi^{-3/4}$.[57] They associate a screening length $\xi(z)$ with the decrease of $\phi(z)$ in a brush so that $\xi(z = 0) = \sigma^{-1/2}$ and it increases with increasing z. Identifying $\xi(z)$ with the blob size, the final blob near the outer end of the brush has a diameter d_{fl} given by the condition that $\xi(z = h - d_{f\ell}) = d_{f\ell}$. This yields $d_{f\ell} = \sigma^{-1/6}N^{2/5}$ and also has been verified by simulations.[44] Therefore, in the scaling limit ($\sigma \to 0$, $N \to \infty$, but $\sigma^{1/3}N$ finite) one needs to distinguish four characteristic lengths to characterize the static structure of a polymer chain in a brush, under good solvent conditions: the blob size $\sigma^{1/2}$ near the wall, the size of the last blob d_{fl} over which the parabolic profile is smeared out, and the linear dimensions R_{gz} and $R_{g\|}$ which all scale with different powers of N and σ (the relations $h \propto R_{gz} \propto \sigma^{1/3}N$ and $R_{g\|} \propto \sigma^{-1/12}N^{1/2}$ are valid even though the Alexander uniform blob picture does not hold, and actually have been confirmed by simulations[38–47]). However, the scaling behavior of the profiles implied by Equation (6), (7), can only be seen if $d_{f\ell}/h \ll 1$ which also can be written as $N^{3/5} \gg \sigma^{-1/2}$, meaning that on the scale of the mushroom size the number of grafting sites must be very large, although σ is very small. This limit is not easily reached in simulations or experiments.

Despite these caveats about the picture of the ''Alexander brush''[11] and the scaling concepts built on it, we shall nevertheless use it as a starting point for a discussion of brushes in cylindrical geometry in the next section.

Chains Grafted Inside of Cylindrical Pores: Theoretical Considerations

While for a chain in a brush on a flat substrate it was plausible[11] to describe it as a linear string of blobs of equal size, the

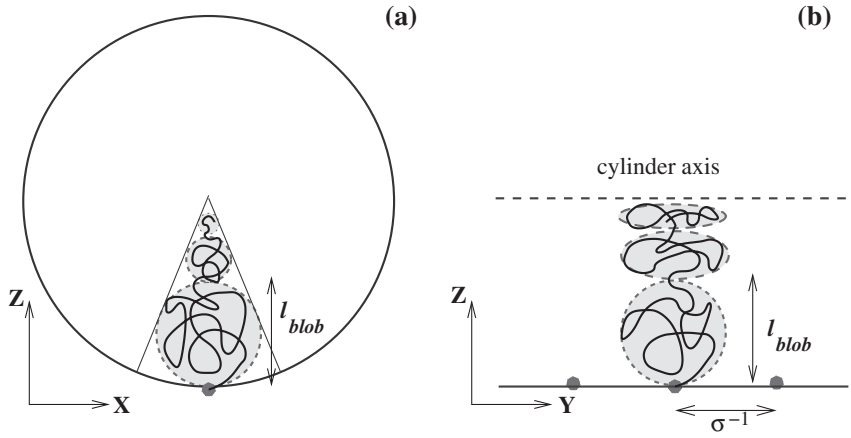

Figure 2.
Schematic illustration of the generalization of the Alexander-De Gennes blob picture for brushes to cylindrical geometry, as proposed by Halperin et al[23,30] and Sevick.[33] It is implied that each chain occupies in the *zx*-plane (cross section of the cylinder) a conical sector (a), with the size l_{blob} of the outermost blob being determined by the grafting density. In the *zy*-plane containing the cylinder axis, all blobs have a linear dimension l_{blob} along the *y*-direction, but become progressively smaller in the *z*-direction toward the cylinder axis (b).

reduction of space resulting from the division of a cylinder into conical sectors implies that then the blob size must get smaller as one gets closer to the center (Figure 2). Thus, the grafted layer is envisioned as a stratified array of blobs in a densely packed arrangement. The blobs within a given concentric shell have all equal size, and any single grafted chain contributes one blob to each shell. In view of the fact that the Alexander brush Picture [11] was found far too simplified, as far as polymer brushes on flat substrates are concerned, it is *a priori* questionable that this generalization is accurate, although it is widely used (e.g.,[23,30,33]) and will also be the starting point of the present discussion. A crucial point, however, is the extension from a strictly linear string of blobs in one direction {Equation (3)} to allow for a random walk behavior in the directions transverse to the *z*-direction, along which the stretching of the chains occurs. In this way, we can also describe a crossover from mushrooms to cigars, that is expected when the diameter of the cylindrical pore becomes comparable to (or even smaller than) the size of a mushroom. In this case we expect that the free end of the chain can be far away from the coordinate $y = 0$ of the grafting site. This is exactly what one sees in the simulations.[51]

It turns out[51] that for chains endgrafted inside cylindrical pores (or nanotubes, respectively) many states compete with each other, depending on the pore diameter D, the chain length N, and the grafting density σ: mushrooms, brushes, cigars,[58,59] compressed cigars. There is also a regime of a brush compressed in *z*-direction, and a regime resembling a semi-dilute solution in the bulk, where there are so many cigars that they must strongly overlap with each other (Figure 3). The dividing lines between these various regimes are not sharp boundaries, of course, but rather smooth crossovers.

This diagram looks rather complicated, but actually the arguments on which it is based are very simple. For instance, we have seen that a brush on a flat surface has the height $h = \sigma^{1/3}N$. If the pore diameter D is very large, the curvature of the brush substrate will not change this result qualitatively, and so we still expect that $R_{gz} = \sigma^{1/3}N$ (apart from factors of order unity). However, when $R_{gz} = D$, this result must break down, since then the brush does

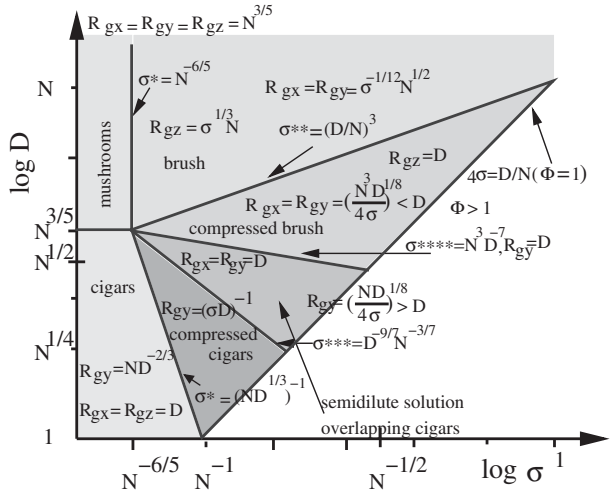

Figure 3.

Schematic diagram showing the linear dimensions of a chain of length N as a function of the pore diameter D and grafting density σ. Straight lines indicate the crossovers between the various scaling regimes. For wide tubes ($D > N^{3/5}$) with increasing σ only two crossovers are encountered, namely at $\sigma = \sigma^* = N^{-6/5}$ from a mushroom to a brush (as at a flat substrate) and at $\sigma^{**} = (D/N)^3$ to a compressed brush. The latter regime ends at $\sigma = (1/4)D/N$, where the pore is densely filled with monomers ($\phi = 1$ cannot be excluded). The line corresponding to $\phi = 1$ meets the line σ^{**} at $D = N$: for $D > N$ no compressed brushes exist any longer. For narrow tubes, $D < N^{3/5}$, in the dilute regime one has cigars instead of mushrooms. These cigars are elongated along the y-axis, $R_{gy} = ND^{-2/3}$. Three subregimes need to be distinguished: for moderately narrow pores, $N^{1/2} < D < N^{3/5}$, three successive crossovers occur. At $\sigma = \sigma* = (N/D^{1/3})^{-1}$ a crossover from swollen cigars to compressed but non overlapping cigars, at $\sigma^{***} = D^{9/7}N^{3/7}$ these cigars start to overlap strongly, but for $\sigma < \sigma^{****} = N^3D^{-7}$ their linear dimension in y-direction still exceeds the tube diameter. At σ^{****} the chains behave similar as in a bulk semi dilute solution of the same density and $R_{gx} = D$. For $\sigma > \sigma^{****}$, the regime of the compressed brush is entered. For narrow pores, $N^{1/4} < D < N^{1/2}$, the latter regime no longer exists. For ultranarrow pores, $1 < D < N^{1/4}$, only a single crossover from swollen to laterally compressed cigars is possible.

no longer "fit" into the pore at all. Equating $R_{gz} = \sigma^{1/3}N = D$ yields $\sigma^{**} = (D/N)^3$. The line $\phi = 1$ is also trivial to understand: it means the tube is densely filled with monomers, the region $\phi > 1$ simply is unphysical. Likewise, the grafting density cannot exceed unity also, then the pore walls would be densely covered with grafted chains. Also the pore diameter cannot be less than unity, in units of the size of effective monomers: then a confined polymer chain would be stretched out like a rigid rod of length N along the y-axis, and this is what the expression for R_{gy} of compressed cigars as well as of ordinary cigars yields in this limit.

Note that for ultrathin pores, $D < N^{1/4}$, only cigars and compressed cigars can exist, and only when D exceeds $N^{1/2}$ can we have compressed brushes.

Particularly interesting is the crossover line $\sigma^{****} = N^3D^{-7}$: along this line, all three linear dimensions R_{gx}, R_{gy}, R_{gz} are of the same order, namely of the order of the pore diameter D. This is the dividing line between cigar-like and brush-like states. And there is one point where no less than six crossover lines meet: the immediate vicinity of this point is the region where for $N \to \infty, \sigma \to 0, D \to \infty$ the scaling description holds! While the linear dimensions of the chains depend on three variables N, σ, D in the general case, in the scaling limit a reduced description holds, where the N-dependence can be completely absorbed in the scaled variables $\tilde{R}_{g\alpha} = R_{g\alpha}/N^{3/5}$. Here α stands for x, y, z and $\tilde{D} = D/N^{3/5}$, while $\tilde{\sigma} = \sigma N^{6/5} = \sigma/\sigma^*$ is the scaled grafting density. For $\tilde{D} > 1$, only two crossovers occur in the scaling limit (Figure 4), from

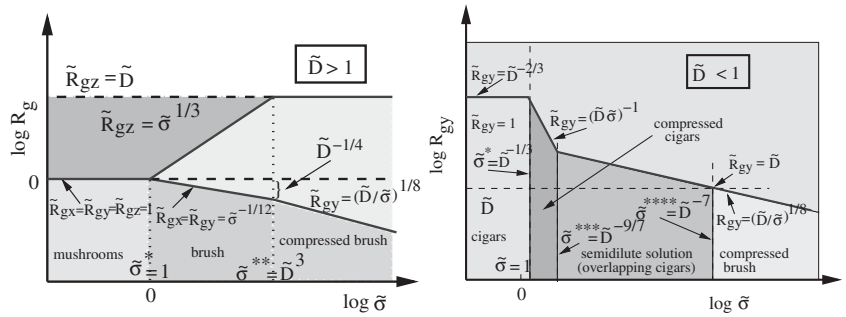

Figure 4.
Schematic variation of the scaled linear dimensions $\tilde{R}_{gx} = R_{gx}/N^{3/5}$, $\tilde{R}_{gy} = R_{gy}/N^{3/5}$, and $\tilde{R}_{gz} = R_{gz}/N^{3/5}$ with the scaled grafting density $\tilde{\sigma} = \sigma N^{6/5}$ on a log-log plot. For wide pores ($\tilde{D} > 1$, upper part) and moderately narrow pores ($\tilde{D} < 1$, but $D > N^{1/2}$, lower part) there is no longer any dependence on chain length N. Since the crossovers at the various grafting densities $\tilde{\sigma}^*$, $\tilde{\sigma}^{**}$, $\tilde{\sigma}^{***}$and $\tilde{\sigma}^{****}$ shown in the figure are not sharp, the dashed vertical straight lines should be understood as centers of crossover regions only.

mushroom to brush and then to compressed brush. When $\tilde{D} < 1$, one starts with cigars (Figure 4), and encounters three crossovers (to compressed cigars, then overlapping cigars, and finally the compressed brush again).[51]

Molecular Dynamics Results for Brushes in Cylindrical Pores

It is clear that from the above scaling description one only gets a qualitative guidance on the behavior of brushes in cylindrical pores in the asymptotic limit of very long chains (and pores that are very wide, in comparison with the size of effective monomers). A much more detailed insight can be derived from computer simulation, although only relatively small systems are accessible.

For our simulations, we use a well-established model,[54–56] namely the bead-spring model where non-bonded beads have a Lennard-Jones interaction U_{LJ} (r),

$$U_{LJ} = 4\epsilon[(\sigma/r)^{12} - (\sigma/r)^6] + 127\epsilon/4096\,, \quad r < r_c \tag{9}$$

with $r_c = 2 \times 2^{1/6}\sigma$, $U_{LJ}(r \geq r_c) = 0$, and units now are chosen such that $\sigma = 1$, $\epsilon = 1$. The monomers bonded to each other as nearest neighbors along a chain interact also with the finitely extensible nonlinear elastic (FENE) potential,

$$U_{FENE} = -15\epsilon(R_0/\sigma)^2 \log(1 - r^2/R_0^2), \quad R_0 = 1.5\sigma \tag{10}$$

This model provides a very good description of both polymer solutions and melts. The Θ-temperature occurs for $\Theta = 3.3$[56] ($k_B = 1$), and in order to work in the good solvent regimes, we choose $T = 4$.

Figure 5 shows typical radial density profiles. Note that the first monomer of each chain has been fixed at a rigid position at distance $\Delta z = 1$ from the wall at the inside of the nanopore: therefore there is a delta function spike in Figure 5a at this distance. The next peak is due to the layering effect of fluids near hard walls, as in the case of the brush at the flat substrate (Figure 1).

One can see that for not too large N, where hardly any monomers are near the pore center at $r = 0$, the profiles $\phi(r)$, $\rho(r)$ resemble that of brushes at flat substrates. Again the generalization of the Alexander picture (due to Sevick[33] and others), implying that $\rho(r)$ is a delta function at the brush height, $\rho(r) \propto \delta(r - (R - h))$ is a poor approximation.

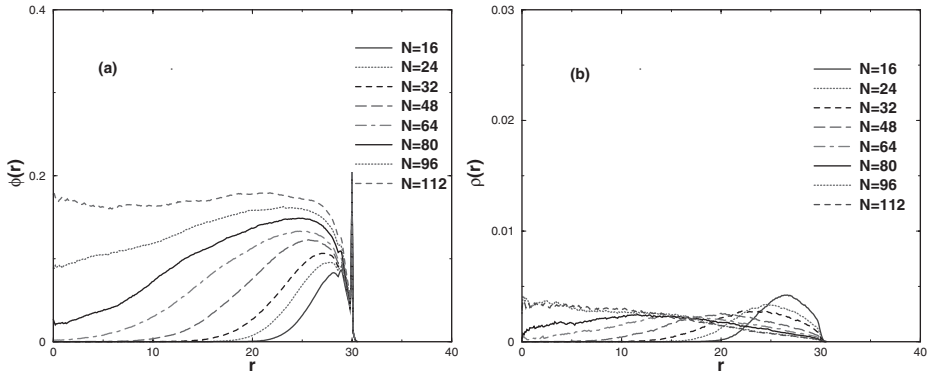

Figure 5.
Radial density distribution $\phi(r)$ of the monomers as a function of the distance r from the cylinder axis, for a pore of radius $R = 31$, at a grafting density $\sigma = 0.0755$, i.e. using $N_{ch} = 960$ chains (a), and the corresponding end monomer distribution (b). At $r = R - 1 = 30$ the first monomer of each grafted chain is located at a fixed position, while the particles forming the wall are located at $r = R = D/2 = 31$.

When N is large so that the monomers extend also to the region near the center of the pore, the distributions $\phi(r)$, $\rho(r)$ differ qualitatively from those shown in Figure 1: now $\phi(r)$ is nonzero at $r = 0$, and $\rho(r)$ even is maximal there. However, this special behavior is just a consequence of the fact that by recording a radial distribution some important information on the conformation of the chains is lost, see Figure 6. When one defines a new coordinate r' that distinguishes in which hemicylinder a monomer is, as explained in Figure 6, one again obtains smooth distributions with no sin-

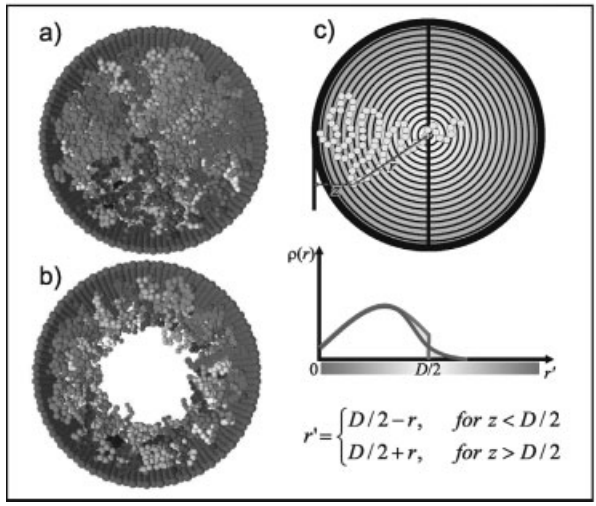

Figure 6.
(a) Snapshot picture of a polymer brush with $R = 14, N = 48, \sigma = 0.0341$ (b) Snapshot picture for $R = 14, N = 16, \sigma = 0.0341$. (c) Schematic configuration of a chain extending with some monomers out of the hemicylinder containing the grafting site. (d) Schematic construction of a distribution $\rho(r')$ that distinguishes to which hemicylinders the monomers belong: $r' = D/2 - r$ for $z < D/2$ while $r' = D/2 + r$ for $z > D/2$.

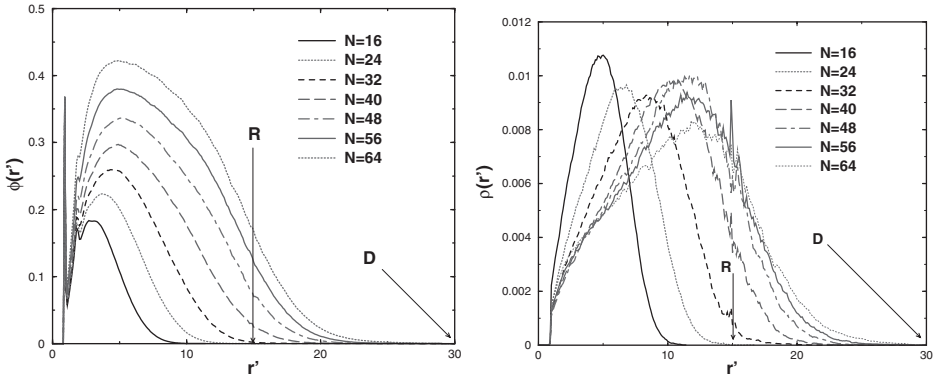

Figure 7.
Density profile $\phi(r')$ of the monomers (a) and chain end distribution $\rho(r')$ (b) for the case $D = 30$, $\sigma = 0.02$ and various chain lengths. Arrows point to the cylinder axis (labeled by *R*) and to the maximum distance in the pore (*D*), respectively.

gularity at a distance $r' = R = D/2$ corresponding to the pore center - Figure 7. These distributions now again look similar to their counterparts for brushes on flat substrates. Thus, unlike the blob hypothesis suggestions, Figure 2, chains do not stay confined within their conical compartments, but actually the chains may share collectively a much larger volume available inside the pore.

When one compares these profiles for otherwise identical conditions while varying D, one finds that with increasing the curvature $1/D$ the profile initially gets broader and hence h initially increases with $1/D$ - cf. Figure 8, inset. This is in contrast with the results of Sevick[33] who obtained a monotonous decrease of h with $1/D$. Of course, the increase of h with $1/D$ must stop when one starts to fill the pore center with monomers, and h reaches a saturation value near $D/2$. This is clearly seen when one studies the variation of h with N for small D, when one crosses over from the approximately linear increase $h \propto N$ to a saturation value independent of N, Figure 8.

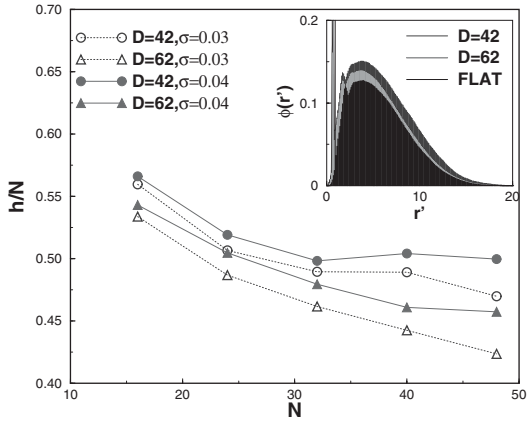

Figure 8.
Brush height h plotted versus N for various diameters D and grafting densities σ, as indicated. Inset compares the density profiles $\phi(r')$ versus r' for two choices of D at $\sigma = 0.03$ with the monomer density profile of a flat brush.

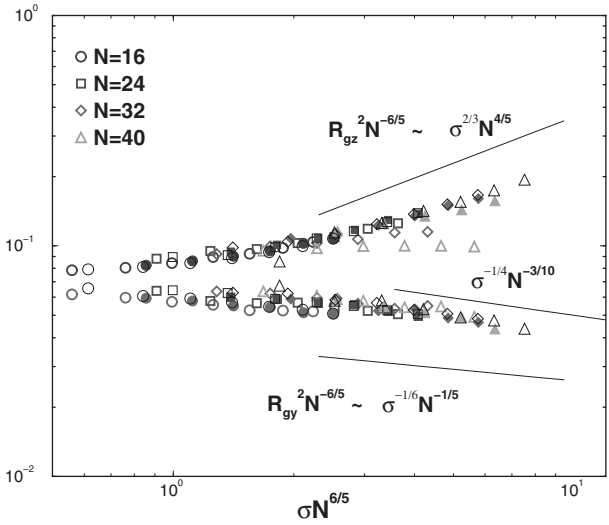

Figure 9.
Scaling representation where $\langle \tilde{R}_{gz}^2 \rangle$, upper part, and $\langle \tilde{R}_{gy}^2 \rangle$, lower part, are plotted vs. the scaling variable $\tilde{\sigma} = \sigma N^{6/5}$, in the double-logarithmic forms, including data for various N (as indicated in the figure) and three choices of D (open symbols, thick small: $D = 30$, thin big: $D = 62$; full symbols: $D = 42$). Predicted power laws for the brush regime and the compressed brush regime are shown by straight lines.

When one studies the chain gyration radius components considered in Figure 3 for the present model, one rarely finds clear power laws exhibiting the theoretical values, but rather one finds on the log-log plot ''effective exponents'' in between the theoretical values,[51] reflecting smooth crossovers from one regime to the other. Therefore in a scaling plot, suggested by Figure 4, one observes neither clearcut data collapse nor straight lines with the predicted slopes (Figure 9). Rather one observes a gradual crossover, and there are also pronounced corrections to scaling present, which is not surprising, since the available chain lengths N are rather small. Note that $\tilde{D}$ also varies here, since we have worked with three constant values of D rather than with a fixed $\tilde{D}$. However, it is also clear that real cylindrical pores in which chains could be grafted (e.g. artificial nanochannels which have a width between 35 and 150 nm[60] and are used for studying confined DNA[61]) would hardly allow to study the scaling limit ($N \to \infty$, $\sigma \to 0$, but $\sigma^{1/3}$ N large) either.

Concluding Remarks

The configurations of flexible macromolecules endgrafted at the inner surface of a cylindrical nanotube or pore pose challenging problems, since the chain stretching (caused by excluded volume interactions when the grafting density is high enough, so that mushroom-type configurations would overlap strongly, i.e. $\sigma \gg \sigma* = N^{6/5}\sigma$), competes with chain confinement.

We have found in the region where the brush height h is still much smaller than the cylinder radius $R = D/2$ that the height on such a curved substrate is slightly *larger* than for a brush on a flat substrate (Figure 8). This conclusion disagrees with results due to Sevick[33] based on a simple extension of the Alexander brush model to cylindrical geometry, but it agrees with expectations based on the strong stretching limit of self-consistent field theory.[36] However, the appropriate formulation of ''blob pictures'' and self-consistent field theories for cylindrical geometry is subtle and still a matter of ongoing research.[37] In

the regime accessible to the simulations, the idea that the distribution function of chain ends is close to a delta function at the brush height, $\rho \propto \delta(h-r)$, clearly is not valid. Also the basic idea of the Daoud-Cotton-like blob pictures,[62] partitioning space into sectors such that the cylinder is represented as a dense-packed arrangement of blobs (Figure 1), and each chain is confined to the conical sector containing the grafting site, does not hold: chains are not confined to the resulting compartments (that would look like a piece of cake), but rather configurational entropy favors that the chains share collectively a much larger volume, and hence it happens that monomers of a chain are also found in the hemicylinder that does not contain the grafting site (Figure 5–7).

Extending previous scaling treatments,[36] we have derived the asymptotic power laws for the various components of the gyration radius of the chains as function of grafting density σ, chain length N and pore diameter D (Figure 3). We have found that in addition to the states of mushroom and brush, familiar from flat substrates, many additional states of the chains exist: compressed brushes, swollen and compressed cigars, and overlapping cigars resembling a semidilute solution. The scaling description, (Figure 4, where the N-dependence is absorbed in suitably scaled variables ($\tilde{\sigma}$,$\tilde{D}$, etc.) could only be verified rather roughly (Figure 9), due to smooth crossovers and corrections to scaling. We expect that also in practically relevant cases the asymptotic region where scaling holds ($\sigma \to 0$, $N \to 0$ such that $N\sigma^{1/3} \gg 1$) will hardly be reached and hence the behavior of real systems should resemble the results from our simulations.

However, there is one other problem that should be noted: in many real systems there is one more relevant variable, namely the quality of the solvent. This can be quantified by the strength of the excluded volume interaction, or (alternatively) the distance from the Θ-point.[57] This leads to a correlation length for the thermal crossover[57] and it now matters whether or not this length exceeds the blob size at the wall.[50] The consequence of this fact is that even for the scaling description of a polymer brush at a flat wall a single scaling variable $N\sigma^{1/3}$ does not suffice, but rather two scaling variables $X = \sigma N$, $Z = v_{ex}N^{1/2}$, where v_{ex} measures the strength of the excluded volume potential, are required, and the simple scaling description alluded to here works only[50] for $X \ll Z^2$. The consequences of this problem for brushes in cylindrical geometry have not yet been explored.

Acknowledgements: One of us (D.I.D.) thanks the Max Planck Society for support via Max Planck fellowship. We are also grateful to the Deutsche Forschungsgemeinschaft (DFG) for support under the project No 436 BUL 113/130.

[1] G. Hadziioannou, S. Patel, S. Granick, M. Tirrell, *J. Am. Chem. Soc.* **1986**, *108*, 2869.
[2] S. S. Patel, M. Tirrell, *Annu. Rev. Phys. Chem.* **1989**, *40*, 597.
[3] A. Auroy, L. Auvray, L. Leger, *Macromolecules* **1991**, *24*, 2523.
[4] J. B. Field, C. Toprakcioglu, L. Dou, G. Hadziioannou, G. Smith, W. Hamilton, *J. Phys. II (France)* **1992**, *2*, 221; S. M. Baker, G. S. Smith, D. L. Anastassopoulos, C. Toprakcioglu, A. A. Vradis, D. G. Bucknall, *Macromolecules* **2000**, *33*, 1120.
[5] M. S. Kent, L.-T. Lee, B. Farnoux, F. Rondelez, *Macromolecules* **1992**, *25*, 6240.
[6] H. Watanaba, M. Tirrell, *Macromolecules* **1993**, *26*, 6455.
[7] J. Klein, *Annu. Rev. Mat. Sci.* **1996**, *26*, 581.
[8] L. Leger, E. Raphael, H. Hervet, *Adv. Polymer Sci.* **1999**, *138*, 185.
[9] "*Polymer Brushes*", R. C. Advincula, W. J. Brittain, K. C. Caster, J. Rühe, Eds., Wiley-VCH, Weinheim **2004**.
[10] A. N. Semenov, *Sov. Phys. JETP Lett.* **1985**, *61*, 733.
[11] S. Alexander, *J. Phys. (France)* **1977**, *38*, 983.
[12] P. G. de Gennes, *Macromolecules* **1980**, *13*, 1069.
[13] A. M. Skvortsov, A. A. Gorbunov, V. A. Pavlushkov, E. B. Zhulina, O. V. Borisov, V. A. Pryamitsyn, *Polymer Sci. USSR* **1988**, *30*, 1706.
[14] S. T. Milner, T. A. Witten, M. E. Cates, *Macromolecules* **1988**, *21*, 2610.
[15] S. T. Milner, T. A. Witten, *J. Phys. (France)* **1988**, *49*, 1951.
[16] T. Cosgrove, T. Heath, B. van Lent, F. Leermakers, J. M. H. M. Scheutjens, *Macromolecules* **1988**, *20*, 1962.
[17] E. B. Zhulina, V. A. Pryamitsin, O. V. Borisov, *Polym. Sci. USSR Ser. A* **1989**, *31*, 205.

[18] S. T. Milner, Z. G. Wang, T. A. Witten, *Macromolecules* **1989**, *22*, 489.
[19] E. B. Zhulina, O. V. Borisov, V. A. Pryamitsin, *J. Colloid Interface Sci.* **1990**, *137*, 495.
[20] B. van Lent, R. Israels, J. M. H. M. Scheutjens, G. J. Fleer, *J. Colloid Interface Sci.* **1990**, *137*, 380.
[21] S. T. Milner, *Science* **1991**, *251*, 905.
[22] P. Y. Lai, A. Halperin, *Macromolecules* **1991**, *24*, 3704.
[23] A. Halperin, M. Tirrell, T. P. Lodge, *Adv. Polymer Sci.* **1991**, *100*, 31.
[24] R. C. Ball, J. F. Marko, S. T. Milner, T. A. Witten, *Macromolecules* **1991**, *24*, 693.
[25] E. B. Zhulina, O. V. Borisov, V. A. Pryamitsin, T. M. Birshtein, *Macromolecules* **1991**, *24*, 140.
[26] C. M. Wijmans, J. M. H. M. Scheutjens, E. B. Zhulina, *Macromolecules* **1992**, *25*, 2657.
[27] C. M. Wijmans, E. B. Zhulina, *Macromolecules* **1993**, *26*, 7214.
[28] N. Dan, M. Tirrell, *Macromolecules.* **1993**, *26*, 637.
[29] C. M. Wijmans, E. B. Zhulina, G. J. Fleer, *Macromolecules* **1994**, *27*, 3238.
[30] A. Halperin, in: "*Soft Order in Physical Systems*", Y. Rabin, R. Bruinsma, Ed., Plenum Press, New York **1994**, Vol. *323*, of Series B, Physics, p. 33–56.
[31] I. Szleifer, M. Carignano, *J. Chem. Phys.* **1995**, *102*, 8662.
[32] I. Szleifer, M. Carignano, *Adv. Chem. Phys.* **1996**, *94*, 165.
[33] E. M. Sevick, *Macromolecules* **1996**, *29*, 6952.
[34] C. Hiergeist, R. Lipowsky, *J. Phys. II (France)* **1996**, *6*, 1465.
[35] R. R. Netz, M. Schick, *Macromolecules* **1998**, *31*, 5105.
[36] M. Manghi, M. Aubuouy, C. Gay, C. Ligoure, *Eur. Phys. J. E* **2001**, *5*, 519.
[37] E. B. Zhulina, T. M. Birshtein, O. V. Borisov, *Eur. Phys. J. E* **2006**, *20*, 243.
[38] M. Murat, G. S. Grest, *Macromolecules* **1989**, *22*, 4054.
[39] A. Chakrabarti, R. Toral, *Macromolecules* **1990**, *23*, 2016.
[40] P.-Y. Lai, K. Binder, *J. Chem. Phys.* **1991**, *95*, 9288.
[41] M. Murat, G. S. Grest, *Macromolecules* **1991**, *24*, 704.
[42] P.-Y. Lai, K. Binder, *J. Chem. Phys.* **1992**, *97*, 586.
[43] G. S. Grest, M. Murat, *Macromolecules* **1993**, *26*, 3108.
[44] J. Wittmer, A. Johner, J.-F. Joanny, K. Binder, *J. Chem. Phys.* **1994**, *101*, 4379.
[45] K. Binder, P.-Y. Lai, J. Wittmer, *Faraday Discuss.* **1994**, *98*, 97.
[46] G. S. Grest, *Macromolecules* **1994**, *27*, 418.
[47] G. S. Grest, M. Murat, in: "*Monte Carlo and Molecular Dynamics Simulations in Polymer Science*", K. Binder, Ed., Oxford Univ. Press, New York **1995**, p. 476.
[48] G. S. Grest, *Phys. Rev. Lett.* **1996**, *76*, 4979.
[49] G. S. Grest, *Adv. Polymer Sci.* **1999**, *138*, 149.
[50] T. Kreer, S. Metzger, M. Müller, K. Binder, J. Baschnagel, *J. Chem. Phys.* **2004**, *120*, 4012.
[51] D. I. Dimitrov, A. Milchev, K. Binder, *J. Chem. Phys.* **2006**, *125*, 034905.
[52] D. I. Dimitrov, A. Milchev, K. Binder, D. W. Heermann, *Macromol. Theory. Simul.* **2006**, *15*, 573.
[53] A. D. Sokal, in: "*Monte Carlo and Molecular Dynamics Simulations in Polymer Science*", K. Binder, Ed., Oxford Univ. Press, New York **1995**, p. 47.
[54] G. S. Grest, K. Kremer, *Phys. Rev. A* **1986** *33*, 3628.
[55] C. Bennemann, K. Binder, W. Paul, B. Dünweg, *Phys. Rev. E* **1998**, *57*, 843.
[56] M. Müller, L. G. MacDowell, *Macromolecules* **2000**, *33*, 3902.
[57] P. G. de Gennes, "*Scaling Concepts in Polymer Physics*", Cornell University Press, Ithaca, New York **1979**.
[58] M. Daoud, P.-G. de Gennes, *J. Phys. (France)* **1977**, *38*, 85.
[59] K. Kremer, K. Binder, *J. Chem. Phys.* **1984**, *81*, 6381.
[60] Z. N. Yu, H. Gao, W. Wu, H. X. Ge, S. Y. Chou, *J. Vac. Sci. Technol. B* **2003**, *21*, 2874.
[61] W. Reisner, K. J. Morton, R. Rühn, Y. M. Wang, Z. N. Yu, M. Rosen, J. C. Sturm, S. Y. Chou, E. Frey, R. H. Austin, *Phys. Rev. Lett.* **2005**, *94*, 196101.
[62] M. Daoud, J. P. Cotton, *J. Phys. (France)* **1982**, *43*, 51.

